Superradiance at the localization-delocalization crossover in tubular chlorosomes

Rafael A. Molina and Enrique Benito-Matías
Instituto de Estructura de la Materia, IEM-CSIC, Serrano 123, Madrid 28006, Spain

Alejandro Somoza, Lipeng Chen, and Yang Zhao
Division of Materials Science, Nanyang Technological University, 50 Nanyang Avenue, Singapore 639798

We study the effect of disorder on spectral properties of tubular chlorosomes in green sulfur bacteria *Cf. aurantiacus*. Employing a Frenkel-exciton Hamiltonian with diagonal and off-diagonal disorder consistent with spectral and structural studies, we analyze excitonic localization and spectral statistics of the chlorosomes. A size-dependent localization-delocalization crossover is found to occur as a function of the excitonic energy. The crossover energy region coincides with the more optically active states with maximized superradiance, and is, consequently, more conducive for energy transfer.

PACS numbers: 87.15.M-,73.20.Fz

arXiv:1601.04728v1 [physics.bio-ph] 8 Dec 2015

I. INTRODUCTION

Chlorosomes are the main light-harvesting structures of green sulfur bacteria, some green filamentous anoxygenic phototrophs [1], and the recently discovered aerobic anoxygenic phototroph *Candidatus Chloroacidobacterium thermophilum* [2]. The chlorosomes are self-assembled structures of hundreds of thousands bacteriochlorophyll (BChl) molecules. They differ from other light-harvesting complexes by the absence of a protein matrix which supports the photosynthetic pigments and their very large size with lengths up to 200 nm [3]. Chlorosomes usually function in extremely low light conditions and are thus probably the most efficient light-harvesting antenna complexes in nature [4]. These special properties makes the chlorosome a potential candidate for use in biomimetic light-harvesting devices [5, 6]. Due to the heterogeneity of chlorosomes their structure cannot be determined by crystallographic methods and structural information is scarce. However, thanks to recent advances in different areas, a structural model has been put forward for cholorosomes of the green sulfur bacterium *Chlorobaculum tepidum* [7]. This model is based on a *syn-anti* array of BChl c pigments in tubular shape. One of the methods that were used to determine the structure of the chlorosome was to study mutant bacteria with three genes whose expression was prevented. The mutant bacteria have a more ordered structure of BChls which allowed X-ray crystallographic studies and showed the presence of an helical structure. Interestingly enough, the mutant bacteria growth was much slower than the wild type bacteria. This observation together with the fact that the function of three genes was suppressed in order to make the structure less disordered hints to the possibility that disorder plays a biological function in chlorosomes and a disordered structure is favored by evolution. The obvious role for disorder is the broadening of the optical spectra that in an ordered structure would be too narrow as observed in similar artificial supramolecular structures [7].

However, these results are paradoxical since disorder is also expected to localize the excitonic wave functions and inhibit energy diffusion according to the theory of Anderson localization. Since the seminal paper of Anderson on the absence of diffusion for disordered quantum lattices [8], wave localization due to interference has been a central theme in condensed matter physics. One of the main tools for studying localization phenomena and, in general, disordered quantum systems has been Random Matrix Theory (RMT) [9]. The RMT approach has also been applied to probe thermodynamic properties of closed systems as well as transport properties of open systems. One of the important results in the field is the statistical relationship between the spectral repulsion parameter β and the wave function localization. The β parameter can be used to locate the metal-insulator transtion in three dimensions [10] and it has been shown that there are specific scaling laws between localization and the repulsion parameter in finite, disordered one-dimensional systems [11–14]. Localization in systems with dipolar interactions like the natural light-harvesting complexes have been shown to be much weaker than for the Anderson model with only nearest neighbor coupling [15]. Quantum transport in disordered networks has been extensively studied in connection with its relevance for efficient energy transfer in light-harvesting systems. Centrosymmetry and a dominant doublet spectral structure has been stablished as a general mechanism for highly efficient quantum transport even in the presence of disorder and the natural implementation of this mechanism in the Fenna-Matthews-Olson (FMO) complex of green sulfur bacteria has also been explored [16].

The extraordinary energy transfer properties of chlorosomes are attributed to cooperative phenomena in the BChl aggregates, which are known otherwise as superradiance and supertransfer. Superradiance occurs when a group of emitters, situated at a distance from each other shorter than the wave length of the light, emits coherently with a very high intensity, and was discovered by Dicke in the context of radiating atoms [17]. It has been studied for supramolecular complexes and in the light-

harvesting apparatus of bacterial photosynthesis [18, 19]. In the presence of disorder, static or dynamic, superradiance is quenched, although, in a tight-binding model in a ring superradiance persists for disorder strengths below a critical value even in a regime with strong coupling to the external environment [20]. The optical properties of one-dimensional disordered excitonic systems have been studied extensively, specially in the context of applications to J-aggregates [21, 22]. The localization length of the system has been shown to limit the number of monomers contributing to the superradiance [23]. These results should also apply to supertransfer, a coined term describing non-radiative excitonic transfer of a superradiant patch [24–26]. Supertransfer has been ascribed to play a crucial role in the efficiency enhancement of light-harvesting systems, and in the chlorosome in particular [27, 28]. Photosynthetic systems are arranged in hierarchical structures where energy funnelling from the chlorosome antenna towards the reaction center proceeds throughout a network of superradiant units. Supertransfer refers to the excitation energy transfer (EET) between these superradiant patches. The properties of cylindrical chlorosomes have been studied before in the homogeneous case [29] and in the disordered case [30]. Attempts have also been made at describing the excitonic dynamics in the presence of a bath using a high-temperature, stochastic treatment attributed to Haken and Strobl [31–33].

In this paper, we study the effects of disorder on the localization properties, the spectral statistics and the optical properties, in particular, superradiance, of chlorosomes. We try to give an answer to the previously mentioned paradox. The long range properties of the dipolar interaction between chromophores make the excitonic wave functions more robust against localization. However, for realistic values of disorder and size, there appears a localization-delocalization crossover as a function of the excitonic energy as monitored by the inverse participation ratio and the spectral statistics. Precisely in the low-energy region where there appears more collectiveness in the optical behavior of the states for the clean system, the exciton is more localized when disorder is included. In the presence of static disorder, there is thus a compromise between the collective but localized low energy states (with less nodes in the wave function) and delocalization which happens at high energy. We find that the maximum of superradiance appears at the localization-delocalization crossover and moves to the high energy side of the spectrum as disorder increases. An optimal value of disorder depending on the environmental conditions exists between sufficient superradiance and a wide spectrum that could help explain the energy transfer properties of chlorosomes. The plan of the paper is the following: we present the realistic model for a single rod in Sec. II, the results for the spectral statistics, wave function localization and optical properties are shown in Sec. III and, finally, some conclusions are drawn in Sec. IV with some comments on the possibility of probing experimentally these theoretical results.

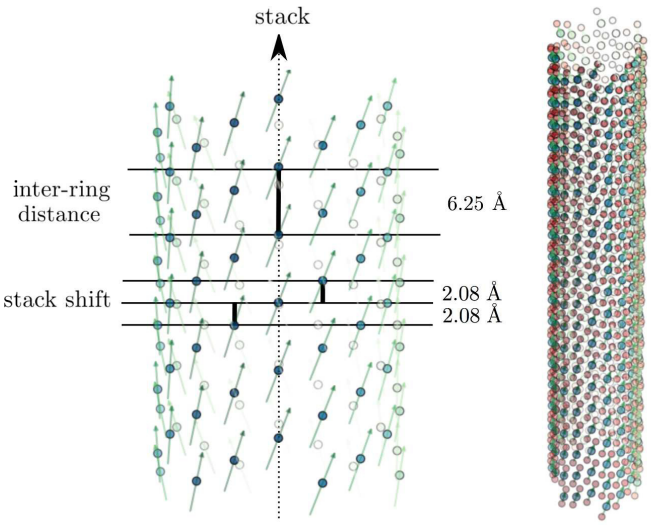

FIG. 1. Sketch of the arrangement of pigments in the chlorosome complex of *Cf. aurantiacus*. The structure is formed by a series of L concentric rings separated by 6.25 Å. A stack is defined as a vertical group of sites, which share the same dipole orientation. The structure has 18 stacks so the total number of sites in the full structure is $N = 18L$. Additionally, there is a vertical shift of 2.08 Å in between adjacent stacks inducing helicoidal pathways in the structure. Each BChl c presents a transition dipole moment (green arrows) which approximately connects two nitrogens (red dots) situated diagonally to the magnesium atom (blue dots) of the chromophore at the center of the pigment.

II. MODEL FOR A SINGLE ROD

We make use of a single rod aggregate structure consisting of a series of L concentric rings in conformance with the model introduced in [34, 35], as shown in Fig. 1. The distance between consecutive rings is 6.25 Å. The structure has 18 different stacks. A stack is defined as a vertical group of sites sharing the same dipole orientation, or equally, the number of sites in one ring. Each ring contains therefore 18 sites and the total number of molecules of the full structure is $N = 18L$. For a certain pigment, the neighbouring sites in the same ring belonging to neighboring stacks present relative heights of -2.08 Å and 2.08 Å with respect to the cylinder symmetry axis. Every pigment in the same stack has the same dipole orientation, forming an angle of 100° with the radius vector connecting the magnesium atom and the symmetry axis and an angle of 36.5° with this axis. Regarding the dipole moments of the pigments belonging to the same ring, neighboring dipole moments are rotated with each other 20° along the symmetry axis. The radius of the cylinder is 21.13 Å (the distance from the magnesium atoms to the symmetry axis). This structure results in

helical pathways of the excitons for energy transfer from the center of the structure to the top or bottom [7, 36, 37].

The excitonic model we use to treat optical properties and localization is based on a model of Frenkel excitons delocalized over a molecular lattice.

$$H = \sum_{n,m} J_{nm} a_n^\dagger a_m, \tag{1}$$

where J_{nm} refers to the excitonic coupling among different sites via dipole-dipole interaction, being $J_{nn} = \epsilon_n$ the monomer excitation energy of a single site. The operators $a_n^\dagger$ (a_n) create (destroy) a molecular excitation at site n. As is often the case within the literature of photosynthetic excitons, we will remain in the one-exciton manifold, assuming that at every time there is only one exciton in the system. Due to the high density of pigments within the chlorosome complex, the often used point dipole approximation is not valid in the present regime where the dipole moment lengths are comparable to the distance between different chromophores. A better approximation is given by the extended dipole-dipole interaction [38]. A point dipole is substituted by opposite charges $+\delta$ and $-\delta$ at a finite distance l:

$$J_{nm} = \frac{D^2}{4\pi\epsilon\epsilon_0 l^2}\left(\frac{1}{r_{++}} + \frac{1}{r_{--}} - \frac{1}{r_{+-}} - \frac{1}{r_{-+}}\right). \tag{2}$$

where $r_{\pm\pm}$ represent the distance between the positive (negative) charge of the point dipole associated with the first molecule to the positive (negative) charge of the point dipole associated with the second molecule. In the case of BChl c pigments the dipole length l is taken to be 8 Å and the squared dipole strength D as 25 Debye^2. The values for the disorder are taken from Ref. [36] and are quoted on Table I. For understanding how disordered the system really is we can compare these values to the parameters of the system. The value for the nearest-neighbor coupling in the system (between adjacent pigments in the same stack) is -282.39 cm^{-1}, the FWHM of the diagonal disorder is 210 cm^{-1} while the FWHM of the nearest-neighbor coupling induced by the non-diagonal disorder is 162.22 cm^{-1}. In the case of the Anderson model with only nearest-neighbor coupling we have verified that the system is fully localized and superradiance is quenched for these values of disorder and for the realistic typical sizes of the chlorosomes. The situation is quite different for the full dipole-dipole interaction as is presented in the next section. For the nearest-neighbors model we have retained the coupling between adjacent sites in the same stack and ring, being the latter 10 times smaller and of opposite sign than the former, due to their relative dipole orientation.

Disorder	value of FWHM
Exciton diagonal energy	210 cm^{-1}
Position along symmetry axis	0.24 Å
Position along x-axis	0.3 Å
Position along y-axis	0.3 Å
angle between dipole and symmetry axis	10°
angle between dipole and radius-vector	20.6°

TABLE I. Parameters for the disorder used in our work, taken from [36].

III. RESULTS: LOCALIZATION, SPECTRAL STATISTICS AND OPTICAL PROPERTIES

In the absence of disorder, an infinite, pristine system can be diagonalized analytically in the momentum representation, and eigenstates can be labeled with two momenta, the longitudinal one on the symmetry axis of the cylinder with continuous values and the transverse one with discrete values that depend on the number of molecules in each ring. Following Didraga *et al.* [29], it is possible to calculate the absorption spectra from the Bloch states that diagonalize the Hamiltonian in momentum state. There are two peaks that concentrate all the oscillator strength. Most of the oscillator strength is concentrated at the excitonic lower state at energy $E_0 = \omega_0 + \Sigma'_n J(n)$, where ω_0 is the energy of one exciton of an isolated BChl c molecule and $\Sigma'_n J(n)$ represents the sum of all the couplings in site space. The wave function of this state is just a coherent superposition of all dipoles with the same coefficient, it has zero transverse momentum $k_\perp = 0$. The other peak is related to the helical structure of the system, the corresponding states have transverse momentum $k_\perp = \pm 1$. The amplitude in this state is such that the components of the dipoles parallel to the z-axis interfere destructively while the ones perpendicular to the z-axis add constructively (the opposite as in the other case). In the case of a finite system without disorder the helical peak is more fragmented due to the effect of the ending points of the cylinder. Although, the monomers are placed in a three-dimensional cylindrical structure wrapped in itself, the properties of the model are more similar to the properties of a quasi one-dimensional system with dipolar interactions [29, 30]. It is interesting to notice that the clean model of the chlorosome has a centrosymmetric structure that has been argued to be an important ingredient for efficient transport in quantum networks [39–41]. A dominant doublet structure is the other critical ingredient needed for optimal quantum transport [16]. Although, outside the model we are using in this work, it is easy to picture a dominant doublet structure as being also important for the behavior of chlorosomes once the full modelling of the coupling to the reaction center is taking into account.

Didraga and Knoester also studied a case of strong disorder with with $\sigma = 800$ cm^{-1} in addition to a weak-disorder case where disorder can be seen as a perturbation mixing helical states with the low energy peak and fragmenting slightly the oscillator strength. They showed that the excitons dominating the optical properties have anisotropic localization along the helices and that the localization length increased with energy from the bottom

to the center of the band. In their case, however the localization length was always smaller than the typical system size.

In order to study the localization properties of the excitonic system we calculate the inverse participation ratio (IPR) [42] defined by

$$\mathrm{IPR}(E_\alpha) = \frac{1}{\sum_i |\Psi_i^\alpha|^4}, \tag{3}$$

where Ψ_i^α is the amplitude of the excitonic eigenstate with energy E_α on site i. IPR = 1 if the state is localized on only one site, and IPR = N if the wave function is equally distributed among all sites in an N site system. Fig. 2 displays the IPR as a function of the normalized state number k/N for cylinders of different lengths. We notice that for realistic values of disorder the IPR is independent of the aggregate length at the edges of the spectrum and thus, wavefunctions present a localized nature. Therefore, the IPR reveals a localized to delocalized crossover which is also signalled by the spectrum statistics as shown below.

The repulsion parameter is defined by the behaviour of the nearest neighbour spacing distribution near degeneracy: $P(s) \sim s^\beta$ $(s \to 0)$, where $s_\alpha = (E_{\alpha+1} - E_\alpha)$. Integrable systems present a Poissonian profile of the spacing distribution with $\beta = 0$ while chaotic systems show level repulsion, avoiding degeneracies with $\beta \sim 1$. The origin of level repulsion comes from the presence of avoided crossings in systems with symmetry-breaking perturbations. Recently, level repulsion has been experimentally verified in disordered cyanine-dye-based molecular nanoaggregates [43]. In order to study the repulsion parameter β of spectral statistics, we fit the nearest neighbor spacing distribution to the phenomenological Brody distribution [44] which has been used succesfully for similar purposes in many areas related to localization in disordered systems or quantum chaos [45–49]:

$$P(s) = A(\beta+1)s^\beta \exp(-As^{\beta+1}).\ A = \Gamma\left[\frac{\beta+2}{\beta+1}\right]^{\beta+1} \tag{4}$$

where the constant A is needed for proper normalization and Γ is the Gamma function. For localized systems, level repulsion is diminished as neighboring levels tend to localize in non-overlapping spatial regions, $\beta = 0$ and the nearest neighbor spacing distribution is equal to the Poisson distribution $P(s) = \exp(-s)$. In systems of disordered but extended states the form of $P(s)$ can be obtained from RMT and can be approximated by the Wigner-Dyson distribution which is equal to the Brody distribution with $\beta = 1$, $P(s) = (\pi/2)\exp(-\pi s^2/4)$ [9]. The Brody distribution interpolates smoothly between these two limits. Previously to the computation of the $P(s)$, the unfolding of the spectra to unit spacing is needed. The unfolding procedure filters the smooth part of the spectrum by performing a local average on the nearest neighbour distances. We have used a local

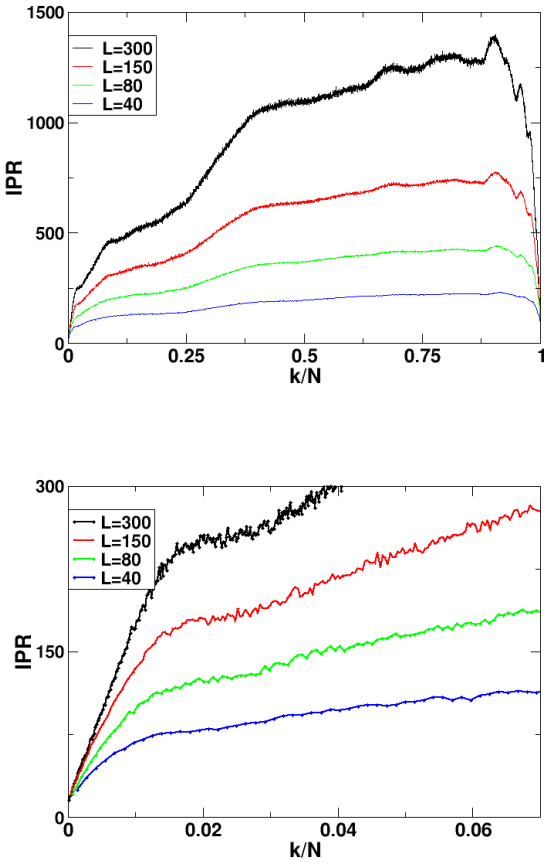

FIG. 2. IPR as a function of the normalized state number k/N for different sizes. The lower panel shows a zoom on the region close to the ground state. We can see how IPR saturates as a function of size for the region close to the ground state up to $k/N \approx 0.005$. Parameters for the disorder are quoted in Table I. The FWHM of the diagonal disorder is 210 cm^{-1} while the FWHM of the nearest-neighbor coupling induced by the non-diagonal disorder is 162.22 cm^{-1}.

unfolding procedure with a window of 5 levels as described in [50]. This procedure describes perfectly well the short range spectral correlations described by the $P(s)$ although it cannot be used to study long range correlations in the spectra [51].

The results are shown in Fig. 3. We show some examples of the fit to the Brody distribution. We have analyzed the data moving a window of 100 levels around some particular level number and analyzing the results every 10 levels (the windows are overlapping). In that way, we can study the repulsion parameter as a function of the exciton energy. The quality of the fit is impressive. The parameter β behaves as a function of the energy in a complementary way to the IPR. This complementarity is tightly related to the sensitivity of the β parameter to the ratio between the localization length and the total length of the system [13, 14]. In the localized region, the

IPR saturates for sufficiently large tubes, indicative of the finite localization length of these states. At higher energies, far from the ground state, the localization length is much longer than the realistic system sizes that we have used (300 rings). For this reason the IPR of Figure 2 increases with larger aggregates in the delocalized region. In contrast, the repulsion parameter decreases as a function of the system size in the localized region, as in that regime β is very sensitive to the ratio between the localization length (which saturates) and the total length of the system. In the delocalized region, β varies very little with the system size although it continues to decrease, albeit slowly. The fact that the repulsion parameter decreases (although very slightly in the middle of the band) as a function of the total length of the chlorosome for all energies is an indication of the localization of the wave functions in the thermodynamic limit, as expected from theoretical considerations [10, 15]. In other words, while the localization length increases with the system size, the ratio localization length / system size tends to zero. For the largest aggregate size we have calculated, the values we find numerically are $\beta \gtrsim 0.6$ in the delocalized region, $\beta \approx 0.5$ in the crossover region and $\beta \lesssim 0.4$ in the localized region of the spectra. The value $\beta \approx 0.5$ corresponds to the energy region where the saturation of the IPR with the system size ceases, giving rise to extended states as shown in the bottom panel of Figure 2. Due to the finite nature of the system, the crossover region is slightly extended around this value.

In general, the excitonic superradiance depends on a variety of controlling parameters, such as temperature, inter-chromophore coupling, static disorder, and various forms of exciton-phonon interactions. For example, the superradiance size is quickly reduced to one with rising temperature. It was also shown that the effect of exciton-phonon coupling on the superradiance size closely resembles that of the static disorder [18]. Here, considering only static disorder, the superradiance size is limited by two factors: 1) it cannot be larger than the localization length; and 2) it cannot be larger than the typical size of the nodal structure (the inverse of the absolute value of the momentum for systems with translational symmetry). In the pristine system when the states are delocalized over the entire system, the localization length is not a limiting factor, and most of the oscillator strength is concentrated in the state with zero momentum. In the disordered case as the localization length increases with energy while the nodal size decreases with energy there will be a maximum of superradiance when the localization length is approximately equal to the nodal size and there is a state with coherence along the whole localization region. As disorder is increased the region with maximum superradiant size moves to higher values of energy up to the point where disorder is so large that superradiance is destroyed and the oscillator strength becomes uniform in energy. In order to study superradiance we concentrate on the linear absorption spectrum that can

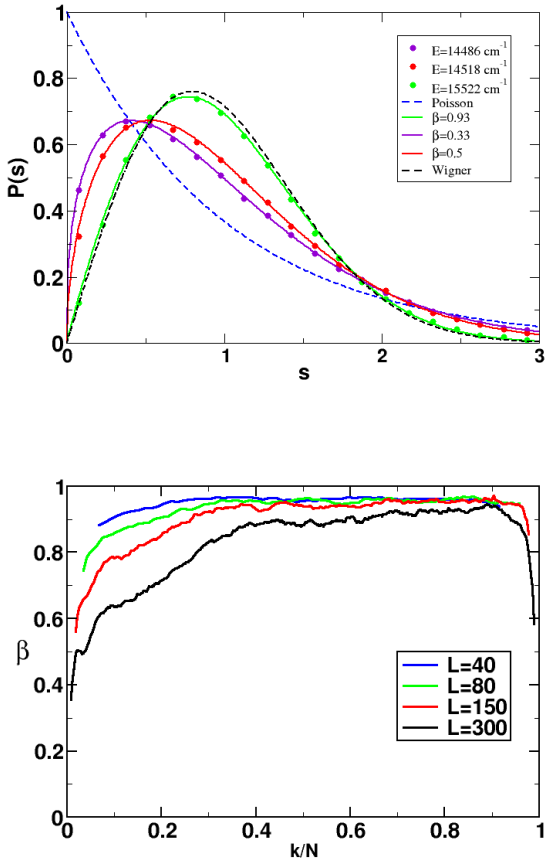

FIG. 3. Top panel: Fit of the $P(s)$ to the Brody distribution in the case of $L = 40, 80, 150, 300$ rings for different values of the central energy of the level window. Bottom panel: Value of β as a function of the renormalized state number k/N for different lengths of cylinder. Parameters for the disorder are the same as in Fig. 2 and are quoted in Table I. The FWHM of the diagonal disorder is 210 cm^{-1} while the FWHM of the nearest-neighbor coupling induced by the non-diagonal disorder is 162.22 cm^{-1}.

be computed in the dipolar approximation through:

$$A(\omega) = \sum_k d_k \delta(\omega - E_k), \tag{5}$$

$$d_k = \left| \sum_n \langle n|\psi_k\rangle \, \boldsymbol{\mu}_n \right|^2 = \sum_{n,m} (c_n^k)^* c_m^k \; \boldsymbol{\mu}_n \cdot \boldsymbol{\mu}_m \tag{6}$$

where d_k is the oscillator strength of excitonic state k, ψ_k is the k excitonic wave function, E_k is the corresponding energy, $|n\rangle$ represents a local excitation at site n, c_n^k is the n-th component of the k excitonic wave function and $\boldsymbol{\mu}_n$ is the dipole vector corresponding to the n molecular dipole in the structure. We assume an isotropic distribution of chlorosomes and average over the direction

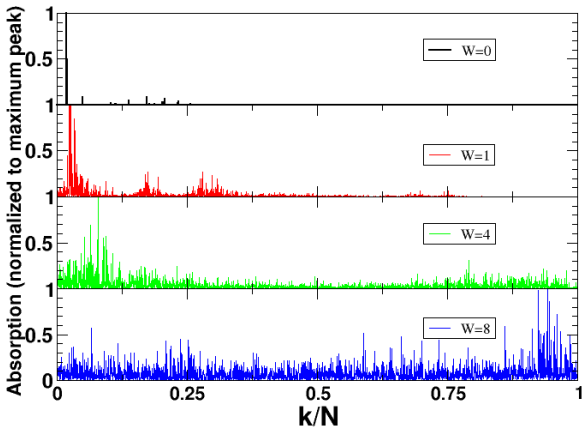

FIG. 4. Stick spectrum for the absorption (normalized to the maximum peak in each case) for four different values of disorder W, a factor multiplying the disorder parameters of Table I (From top to bottom, $W = 0$, $W = 1$, $W = 4$, and $W = 8$). The maximum of the spectrum is moving right with increasing disorder. In the case of $W = 8$ superradiance has been destroyed and the oscillator strength is distributed along all the spectrum, in this particular realization the maximum happens to be by chance closer to the top end of the spectrum. The FWHM of the diagonal disorder is 0 cm^{-1} ($W = 0$), 210 cm^{-1} ($W = 1$), 840 cm^{-1} ($W = 4$), and 1680 cm^{-1} ($W = 8$) while the FWHM of the nearest-neighbor coupling induced by the non-diagonal disorder is 162 cm^{-1} ($W = 1$), 272 cm^{-1} ($W = 4$), and 359 cm^{-1} ($W = 8$). Note that the parameter W multiplies the values of the FWHM for the geometric parameters of the model which does not translate directly in the same scaling of the FWHM of the nearest-neighbor coupling.

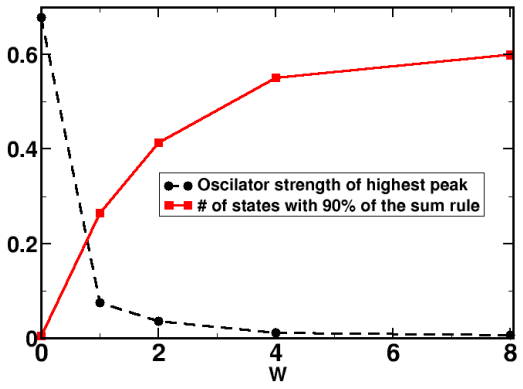

FIG. 5. Oscillator strength of the highest peak in the stick absorption spectrum in units of the sum rule and number of states with a combined oscillator strength of 90% in units of the total number of states as a function of disorder (defined as in the previous figure) for the case of $L = 150$ rings. The result shown is the ensemble average with 1000 realizations of the disorder.

of the polarization vector. We show some examples of the linear absorption stick spectrum as a function of the level number for typical realizations with different disorder strengths in Fig. 4.

We have examined how absorption spectra of the system and spectral statistics are related to superradiance and localization of the wave function. As a measure of the superradiance length as a function of disorder, we have calculated the oscillator strength of the highest peak. In order to measure the fragmentation, we have also calculated the minimum number of states that have a combined oscillator strength equal to 90% of the sum rule (we first order the states in augmenting oscillator strength and sum up to the 90% of the sum rule). In Fig. 5 we show both these measures as a function of the strength of disorder W in units of the parameters of table I. The FWHM of diagonal disorder is then 210 W cm^{-1} while the behavior of the non-diagonal disorder is more complicated as the FWHM of the geometric parameters of the model does not translate directly into a FWHM of the non-diagonal couplings which depend on this geometry (see caption of Fig. 4). We can see that superradiance is important up to a disorder strength of $W \sim 4$ corresponding to a FWHM of the diagonal disorder of 840 cm^{-1} and to a FWHM of the nearest-neighbor coupling of 272 cm^{-1}. Although we have examined only a single rod model for numerical convenience, we expect the results to hold for realistic cholorosomes with many concentric rods.

IV. CONCLUSIONS

Superradiance and supertransfer are two sides of the same coin and key to understand the fast energy transfer in chlorosomes of green sulfur bacteria. We have studied the effect of disorder in superradiance of chlorosomes of *Cf. aurantiacus* using the excitonic model developed recently by Ganapathy *et al.* [7]. The dipolar long-range interaction makes disorder not very effective for localizing the excitonic states for cylindrical chlorosomes. However, using tools of Anderson localization theory and spectral statistics such as the IPR and the repulsion parameter β we have shown that there is a localization-delocalization crossover as a function of the excitonic energy that is seen both in the wave function statistics and in the spectral statistics. This kind of supramolecular aggregates concentrate the optical active energy region at low energies were the collective effects of the coupled molecular dipoles are most important. There is, then, a competition between localization and collectiveness (or state coherence) and the more optical active region where superradiance occurs coincides with the crossover region between localization and delocalization. The results found in this work should be applicable to other different supramolecu-

lar aggregates [52, 53]. These states where the absorption is largest are also the ones expected to dominate the energy transfer. The collective supertransfer effect is still important in spite of disorder and should increase dramatically the single dipole transfer rates. There has been experiments that have shown level repulsion via analysis of the fluoresence spectra in J-aggregates [43, 54]. Similar experiments as a function of the size could be performed for chlorosomes to probe the level repulsion in the optically active region and as a consequence the localization of the wave functions with respect to the total size of the chloromeses. The results should be different in the wild type case, more disordered, than for less disordered mutants.

It would also be very interesting to extend the results obtained to the case of coupling to a thermal environment. Studying the transport and absorption properties of the one-dimensional Anderson model coupled to a bath, it has been shown that the maximal diffusion rate occurs at intermediate coupling strength [33]. These results are reminiscent of our results as a function of the energy. These theoretical observations have been linked to the phenomenom of *momentum rejuventation* apart from the role of dephasing in the destruction of destructive interference leading to Anderson localization [55]. The momentum rejuvenation occurs when classical noise counteracts the depletion of high momentum components of the wave-packet suistaining a broad momentum distribution. Realistic models, such as the one explored in this work, in the presence of a thermal bath should be explored in order to understand better the role of these general design principles [16] in the actual behavior of chlorosomes as light-harvesting complexes.

This work was supported in part by Spanish MINECO project FIS2012-34479, CSIC project I-Link0938, CAM research consortium QUITEMAD+ S2013/ICE-2801, and the Singapore National Research Foundation through the Competitive Research Programme under Project No. NRF-CRP5-2009-04.

[1] Frigaard, N.U. Bryant, D.A. in *Microbiology Monographs*, ed. by J.M. Shively (Springer, Berlin, 2006), pp. 79-114.
[2] Bryant, D.A. *et al.* Candidatus Chloracidobacterium thermophilum: An aerobic phototrophic acidobacterium. *Science* **317**, 523-526 (2007).
[3] Holzwarth, A.R., Griebenow, K., Shaffner, K. A photosynthetic antenna system which contains a protein-free chromophore aggregate. *Z Naturforsch C* **45**, 203-206 (1990).
[4] R.E. Blankenship, *Molecular mechanisms of photosynthesis* (Wiley-Blackwell, New York, 2002).
[5] Modesto-Lopez, L.B., Thimsen, E.J., Collins, A.M., Blankenship, R.E., Biswas, P. Electrospray-assisted characterization and deposition of chlorosomes to fabricate a biomimetic light-harvesting device. *Energy Env. Sci.* **3** 216-222 (2010).
[6] Sridharan, A., Muthuswamy, J., Pizzicone, V.B. Optoelectronic energy transfer at novel biohybrid interfaces using light harvesting complexes from *Chloroflexus aurantiacus*. *Langmuir* **25** 6508-6516 (2009).
[7] Ganapathy, S. *et al.* Alternating *syn-anti* bacteriochlorophylls form concentric helical nanotubes in chlorosomes. *Proc. Nac. Acad. Sci.* **106** 8525-8530 (2009).
[8] P.W. Anderson, Phys. Rev. Absence of Diffusion in Certain Random Latticces **109**, 1492 (1958).
[9] M.L. Mehta *Random Matrices* (Academic Press, Amsterdam, 2004).
[10] Ferdinand Evers and Alexander D. Mirlin, Rev. Mod. Phys. **80**, 1355 (2008).
[11] F. M. Izrailev, J. Phys. A 22, 865 (1989)
[12] F. M. Izrailev, Phys. Rep. 196, 299 (1990).
[13] G. Casati, B. V. Chirikov, I. Guarneri, and F. M. Izrailev, Phys. Rev. E 48, R1613 (1993).
[14] S. Sorathia, F.M. Izrailev, V.G. Zelevinsky, G.L. Celardo, Phys. Rev. E **86**, 011142 (2012).
[15] A. Rodríguez, V. A. Malyshev, G. Sierra, M. A. Martín-Delgado, J. Rodríguez-Laguna, and F. Domínguez-Adame, Phys. Rev. Lett. **90**, 027404 (2003).
[16] M. Walschaers, J. Fernandez-de-Cossio Diaz, R. Mulet, A. Buchleitner, Phys. Rev. Lett. **111**, 180601 (2013).
[17] R.H. Dicke, Phys. Rev. **93** 99 (1954).
[18] T. Meier, Y. Zhao, V. Chernyak, S. Mukamel, J. Chem. Phys. **107**, 3876 (1997).
[19] Y. Zhao, T. Meier, W.M. Zhang, V. Chernyak, S. Mukamel, J. Phys. Chem. B **103**, 3954 (1999).
[20] G.L. Celardo, G.G Giusteri, F. Borgonovi, Phys. Rev. B **90**, 075113 (2014).
[21] E. W. Knapp, Chem. Phys. **85**, 73 (1984).
[22] *J Aggregates*, edited by T. Kobayashi (World Scientific, Singapore, 1996).
[23] H. Fidder, J. Knoester, and D. A. Wiersma, J. Chem. Phys. **95**, 7880 (1991).
[24] W. Strek, Phys. Lett. A **62**, 315 (1977).
[25] S. Lloyd, M. Mohseni, New. J. Phys. **12**, 075020 (2010).
[26] D.F. Abasto, M. Mohseni, S. Lloyd, P. Zanardi, Phil. Trans. R. Soc. A **370**, 3570 (2012).
[27] Joonsuk Huh, S. K. Saikin, J. C. Brookes, S. Valleau, T. Fujita, A. Aspuru-Guzik, J. Am. Chem. Soc. **136**, 2048-2057 (2014).
[28] I. Kassal, J. Yuen-Zhou, S. Rahimi-Keshari, J. Phys. Chem. Lett, **4**, 362 (2013).
[29] C. Didraga, J.A. Klugkist, J. Knoester, J. Phys. Chem. B **106**, 11474 (2002).
[30] C. Didraga, J. Knoester, J. Chem. Phys. **121**, 10687 (2004).
[31] T. Fujita, J. C. Brookes, S.K. Saikin, A. Aspuru-Guzik, J. Phys. Chem. Lett. **3**, 2357 (2012).
[32] J. Ye *et al.*, J. Chem. Phys. **136**, 245104 (2012).
[33] J.M. Moix, M. Khasin, J. Cao, New. J. Phys. **15**, 085010 (2013).
[34] V.I. Prokhorenko, D.B. Steensgaard, and A.R. Holzwarth *Biophys. J.* **79**, 2105 (2000).
[35] The structural parameters are slightly updated. Data provided by Holzwarth A.R. in private communication.
[36] Prokhorenko, V.I., Steensgaard, D.B., and Holzwarth A.R. . *Biophys. J.* **85**, 3173 (2003).

[37] Oostergetel, G. T., van Amerongen, H., Boekema, E.J. The chlorosome: a prototype for efficient light harvesting in photosynthesis *Photosynthesis Research* (2010).
[38] Czikklely V., Forsterling, H., Kuhn, H. *Chem. Phys. Lett.* **6**, 207 (1970).
[39] M. Christandl, N. Datta, T.C. Dorlas, A. Ekert, A. Kay, A.J. Landahl, Phys. Rev. A **71**, 032312 (2005).
[40] A. Kay, Phys. Rev. A **73**, 032306 (2006).
[41] T. Zech, M. Waschaers, T. Scholak, R. Mulet, T. Wellens, A. Buchleitner, Fluct. Noise Lett. **12**, 1340007 (2013).
[42] R.J. Bell, P. Dean, Discuss. Farady Soc. **50**, 55 (1970).
[43] R. Augulis, A.V. Malyshev, V.A. Malyshev, A. Pugžlys, J. Knoester, P.H.M. van Loosdrecht, J. Phys. Chem. Lett. **1**, 2911 (2010).
[44] T.A. Brody, Lett. Nuovo Cimento **7**, 482 (1973).
[45] M. Wilkinson, M. Feingold, L.T. Leitner J. Phys. A: Math. Gen. **14**, 175 (1991).
[46] R.A. Molina, J.M.G. Gómez, J. Retamosa, Phys. Rev. C **63**, 014311 (2000).
[47] J. Flores et al. EPL **101** 67002 (2013).
[48] Frisch *et al.*, Nature (London) **507**, 475 (2014).
[49] J. Mur-Petit, R.A. Molina, Phys. Rev. E **92**, 042906 (2015).
[50] F. Haake *Quantum signatures of chaos* (Springer, Berlin, 2001).
[51] J.M.G. Gómez, R.A. Molina, A. Relaño, J. Retamosa, Phys. Rev. E **66**, 036209 (2002).
[52] Y. Zhao, G. Chen, and L. Yu, J. Chem. Phys. **113**, 6502 (2000).
[53] L. Hu, Y. Zhao, F. Wang, G. Chen, C. Ma, W. Kwok, D. Philips, J. Phys. Chem. B **111**, 11812 (2007).
[54] A.V. Malyshev, V.A. Malyshev, J. Knoester, Phys. Rev. Lett. **98**, 087401 (2007).
[55] Y. Li, F. Carusso, E. Gauger, S.C. Benjamin, New. J. Phys. **17**, 013057 (2015).